33rd European Conference on Acoustic Emission Testing
12-14 September 2018 - Senlis - France

ON USE OF SIGNAL FEATURES FOR ACOUSTIC EMISSION SOURCE IDENTIFICATION IN FIBRE-REINFORCED COMPOSITES

Markus G. R. Sause[1]

[1] University of Augsburg, Institute for Materials Resource Management, Mechanical Engineering, D-86135 Augsburg

Abstract:

In the past, many approaches were proposed to perform the task of acoustic emission based source identification in fibre-reinforced composites. Almost all identification attempts make use of feature values to act as representation of the recorded acoustic emission signals. The typical features are classified in two primary categories, one to express the intensity / energy of the signal and one to describe the frequency characteristic of the signal. Both categories are used to classify signals into microscopic failure mechanisms such as matrix cracking, fibre breakage and many more. To this end, various approaches used either energetic or frequency features or a mix of both. This contribution takes a closer look at the relationship between acoustic emission signals and their feature values and assesses their relation to acoustic emission source mechanics. This provides guidance on the reliability of acoustic emission features for source identification procedures and points out some key aspects for successful classification attempts.

1. Introduction

Failure of composite materials during mechanical loading is a complex phenomenon starting on the microscopic level. At exposure to increased load, small flaws start to grow into larger ones, escalating over several orders of magnitude, which finally coalescent into macroscopic failure. Each microscopic (and macroscopic) crack progression generates acoustic emission (AE). The multitude of different cracks occurring in composites have been categorized and listed several times (i.e. [1], [2]). In the context of AE, it is most noteworthy that all of these different cracks result in detectable AE signals. Among other things, the detectability will depend on the distance between source position and the sensor position. One intrinsic challenge is to deal with the variety of terminology used in the past to categorize the different failure mechanisms in composites. Still there is no consensus on how many different AE source mechanisms can be distinguished in a particular test setup. However, in the past decades there have been many attempts to distinguish between the different AE source mechanism as occurring in composites [3-20]. Basic distinction is made between work that has applied model specimens to establish prototype signals for each source type, approaches that are using validation of signal classes by microscopic evidence and approaches using numerical or analytical modelling to assist in the interpretation.

The aim of this contribution is to review the reliability of particular AE parameters (features) applied to perform source identification in fibre-reinforced composites.

2. Experimental

As described in more detail in [10], [12], a four-point bend test was combined with multi-resonant type WD sensors to detect the AE generated during damage initiation and progression. For acoustic coupling Baysilone silicone grease of medium viscosity was used, the mechanical contact was provided by two clamps. To decrease detection of friction noise a bandpass ranging from 20 kHz up to 3 MHz was used. The AE waveforms were recorded using a PCI-2 data acquisition system with 40 dB_{AE} preamplification and the software AEWin (Physical Acoustic Ltd.) with a threshold of 40dB_{AE} and a sampling rate of 10 MS/s. This will provide some representative AE data for further discussion and only acoustic emission sources located between the two upper supports are considered for the following analysis.

To analyse the crack formation inside the material, high-resolution computed tomography was used. The Nanotom m system (General Electric) was applied with 50 kV tube voltage and 200 µA tube current using a voxel resolution of 5.2 µm. This provides a way of volumetric measurement of the typical crack dimensions found after four-point bending in a composite material.

After extraction of classical signal features out of the first 100 µs after signal arrival (definition of features see Appendix C in [2]), the feature dataset is ready for analysis by pattern recognition methods. In figure 1, a typical result from a hierarchical clustering using the agglomerative tree linkage [21] is shown for one representative dataset resulting from loading the specimens to failure. This statistical data analysis method applies the Ward-algorithm (also known as “sort algorithm” or “agglomerative tree linkage”) and groups the AE features according to their similarity based on a minimum variance criterion [19], [22]–[25]. High numerical values indicate an equal relevance to describe the underlying data structure. In the example of figure 1, the feature “energy” and “signal strength” link at a value of approximately one, so they essentially provide the same information, i.e. they are highly correlated.

For composite materials, this feature dendrogram (example see figure 1) often splits in two branches that link at relatively low levels. One branch is primarily composed of features related to the “energetic quantities”, such as energy, amplitude, signal strength, but it also includes features related to the amplitude. One such example is the duration of the signal (louder signals take longer to fall below threshold). Similar, the rise time and the counts to peak correlate with the strength of the signals as increased amplitudes may cause an earlier onset above threshold level.

The other branch of the feature dendrogram typically holds the features, related to frequency information of the AE signals. Besides the obvious frequency measures, this chart reveals the high correlation between counts and the average frequency, as the latter is based on the former value (see Appendix C in [2] for precise definition).

As this kind of behaviour seems to appear in many AE datasets of composites, this indicates that there is a distinct difference in the descriptive capabilities of both branches. Therefore, this motivates the organization of this work in two sections, one dealing with a review of “energetic” AE features and one dealing with a discussion of “frequency” AE features.

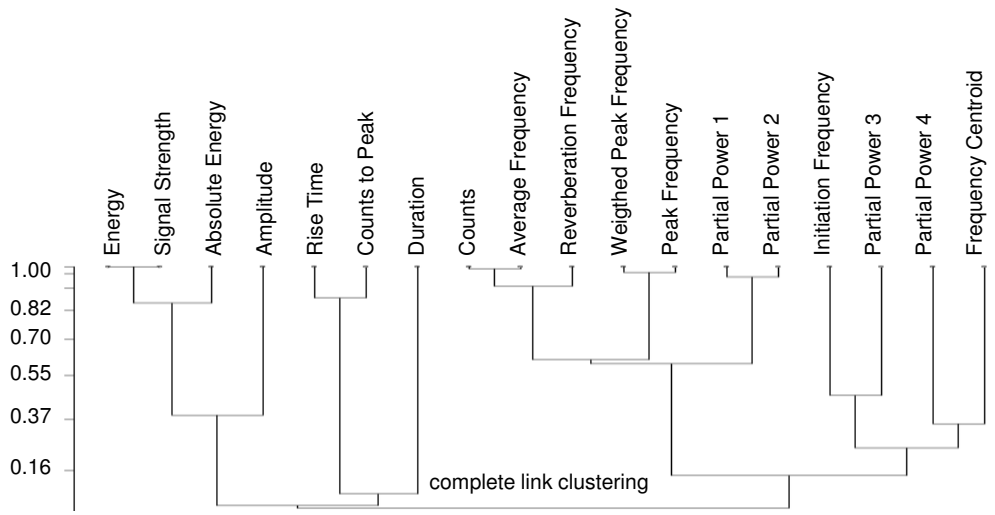

Figure 1. Hierarchical clustering of dataset using the Ward-algorithm (agglomerative tree linkage).

3. Energetic AE signal features

Several fundamental acoustic emission theories aim to establish a relationship between the AE source type, the properties of the fracturing homogeneous isotropic solids and the resulting AE signal [2]. Composite materials are, dependent on the observation scale, significantly different to that, i.e. they are only homogeneous on the macroscopic scale where they may be approximated as homogeneous anisotropic solids. Nevertheless, the key principles of these theories are still found to be still valid for composite materials [2].

One of the common results of all the theories mentioned above is that they expect a proportionality between the size of a crack growth a and the AE signal amplitude U. The theory of Lysak would propose $U \propto a^{3/2}$ for the case of a "crack-through" and $U \propto a$ for an internal "penny-shaped" crack [22]. Green and Zerna reported a $U \propto a$ relationship for a crack-through process [26]. Investigations by finite element modeling recently confirmed the relationship $U \propto a^{3/2}$ for a crack-through process in a homogeneous material, while results from internal cracks apparently obey the $U \propto a$ relationship [2].

The theory of Ohtsu and Ono uses the moment tensor representation for AE sources, which generally states $U \propto \Delta V$, with ΔV being the internal volume produced by the crack growth [23], [24]. Similar, the theory of Scruby and Wadley would predict the proportionality $U \propto \Delta V$, given the dynamics of the crack process are unchanged when comparing different crack sizes [2], [27], [28].

3.1. Matrix cracking and interfacial failure

In a composite, the expected variation of crack sizes for "matrix cracking" ranges from fairly small length scales in the order of 1 µm to 10 µm (cf. figure 2a) to reasonably macroscopic sizes such as several 100 µm to some 1 mm (cf. figure 2b). In [29] polymer fracture was even measured to generate one huge signal for final fracture at several centimetres of length scale.

The theories quoted above allow estimating an increase of the corresponding acoustic emission signal amplitude by three orders of magnitude. This corresponds to a dynamic range of the corresponding AE signal amplitudes of at least 60 dB (1µm to 1mm internal cracks). Furthermore, for a typical composite, there is no expectation of distinct crack sizes, as larger "matrix cracks" do not necessarily need to grow at once, but may show several intermediate rests. This will result in more than one AE signal for one such macroscopic crack. Accordingly, the distribution of crack lengths for source types such as "matrix cracking" and "interfacial failure" is not discrete. This is different in some cases, when the typical extent is geometrically limited in one more directions (e.g. because of ply structure, bundle distances, or other). Thus, in [30] it was demonstrated, that the average signal amplitude of matrix cracking is related to the thickness of the failing plies. Similar, findings in [31] indicate, that matrix cracking in fibre yarns causes characteristic acoustic emission energies.

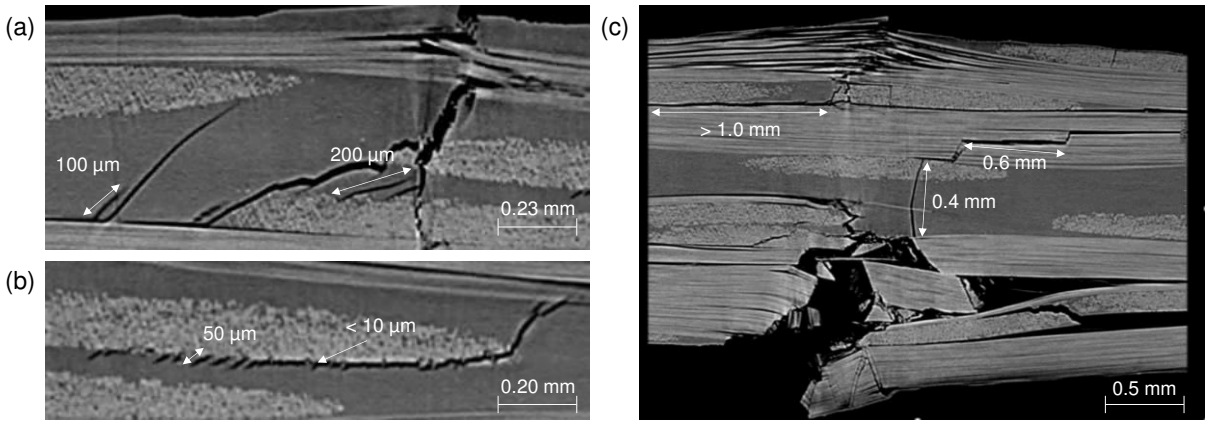

Figure 2. Computed tomography image of crack network on microscale (a and b) and on macroscale (c) taken from damage region of four-point bending sample of [10], [12].

Nevertheless, for the majority of composites, there is no general discretization of crack dimensions for matrix cracking and interfacial failure, but a homogeneous distribution of crack length sizes. Hence, it appears invalid to detect the occurrence of either "matrix cracking" or "interfacial failure" based on a particular amplitude range unless the microstructure explicitly forces discrete size distributions.

3.2. Fibre breakage

Another type of failure mechanism frequently interpreted in terms of its expected AE signal amplitude is fibre breakage. Essentially, contradicting proposals have been made that either concluded $U_{fiber} \gg U_{matrix}$ or $U_{fiber} < U_{matrix}$.

Based on the theories mentioned in section 3.1, the decisive factor for the size of the AE amplitude is the ΔV-value. Due to the fibre diameters, the crack area is well defined for carbon fibres (5 µm to 10 µm) or glass fibres (10 µm to 50 µm). For fibres failing under tensile load, the additional contribution to ΔV is the extension along the fibre axis. The amount of this extension in load direction relates to two factors, namely (i) the amount of elastic energy stored before fibre failure and (ii) the confinement effect of the surrounding fibres and matrix. The first

contribution implicitly relates the amount of extension to such factors as the fibres tensile strength (or their fracture toughness). Hence, a larger ΔV expects for a stronger fibre. In addition, a stronger AE signal is expected for a 10 µm diameter cracking fibre vs. a 10 µm diameter cracking matrix polymer. Assuming typical fibre and matrix failure strength values (50 MPa polymer vs. 5 GPa fibre) and applying the theoretical relationships above, for the same cross-sectional area this results in 100 times larger AE signal amplitude and accordingly $U_{fiber} < U_{matrix}$. Note that this description does not take into account potential additional contributions to ΔV due to matrix cracking and debonding surrounding the fibre filament. This might well lead to additional contributions to the fracture surface normal to the tensile load (i.e. factor of 2 – 4 as estimated from computed tomography images, cf. figure 3).

A primary difference to the discussion of amplitude distribution of section 3.1 is the discrete size distribution expected for fibre breakage. As demonstrated e.g. by [32] the single filament failure initiates long before ultimate failure and does not necessarily result in cascades of fibres failing simultaneously. For constant cross-section and constant fibre strength, a discrete AE energy release is theoretically expected. However, this discrete energy smoothens out due to the cross-section distribution of the fibre filaments and the Weibull strength distribution of the filaments.

Single filament testing sometimes is used to demonstrate that fibre breakage AE signals have very strong amplitudes. As sketched in figure 3, the confinement of the failing filament is substantially different in single filament testing vs. a real composite. In the case of the free filament, the crack faces may move independently in each direction, reaching many millimetres or even centimetres. For fibre failure inside a composite material, the surrounding fibres and matrix (in case they do not fail simultaneously) confine the movement of the breaking fibre. In this case the resulting movement along the axis could be quantified using in-situ computed tomography analysis to be less than 5 µm as seen in figure 3-b [33]. Thus, the resulting ΔV is more than three orders of magnitude smaller than for single filament testing. Based on the theories stated above this would result in a corresponding reduction of AE signal amplitudes of up to 90 dB_{AE}. The same change in energy release was also consistently found in finite element modelling for the case of free fibre filaments in [33] and for confined fibres in [2].

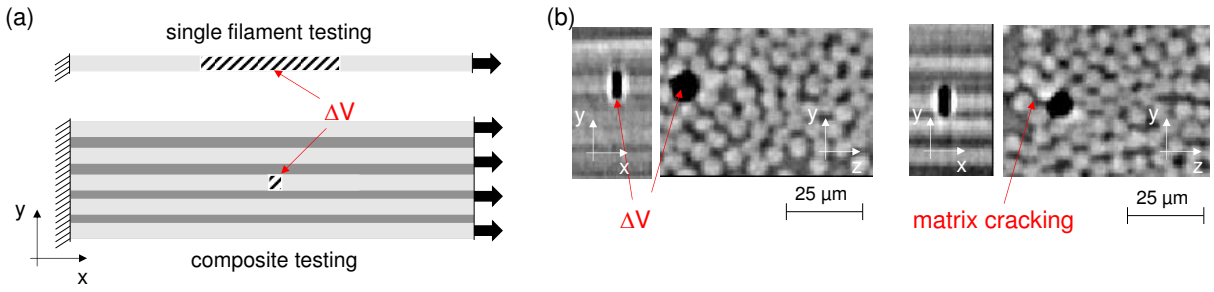

Figure 3. Schematic difference in ΔV for single filament testing vs. fibres confined within composite material (a) and experimental measurement of ΔV using high-resolution computed tomography at 0.4 µm voxel size (b).

Other indications that fibre breakage signals from composites (confined condition) show relatively low amplitudes were recently provided by Lomov et al. and Swolfs et al. [30], [31]. They compared theoretical predictions for first fibre filament failure based on classical Weibull theory to the corresponding onset of AE signals. Overall, the predicted onset of the weakest fibre filaments systematically preceded the measured AE onset. This indicates that the AE signals of the weakest fibres possibly fall below the experimentally used detection threshold. This was additionally verified by finite element modelling of fibre breakage with varying tensile strength following a Weibull-type strength distribution in [2].

As baseline of all these considerations above, the dominating factors for the AE signal amplitude (and hence energy) are the size of the crack as well as the amount of elastic energy stored immediately before fracture.

4. Frequency AE signal features

In contrast to the energetic AE signal features, there are several established ways to compute frequency information to represent the recorded AE signals. The three different features “Initiation-“, “Reverberation-“ and “Average-Frequency” are used to provide an estimate of the characteristic frequency before and after the peak-maximum and of the complete signal (see Appendix C in [2] for precise definition). These features are no exact frequencies since they rely on the number of signal threshold crossings, which is a discrete and often error-prone count, thus resulting in relatively inaccurate nominal frequencies.

A significantly better approach is to compute the Fast-Fourier-Transformation (FFT) of the AE signal. The “Peak-frequency” f_{peak} is the frequency value of maximum intensity in the spectrum. The “Frequency Centroid” $f_{centroid}$ characterizes the frequency content of an AE signal in a similar way as the centre of mass describes the properties of geometric object with uniform density. Thus, it is an independent evaluation of the characteristic average frequency of the signal and is generally not equal to the “Peak-frequency”. Another means of representing the signals frequency spectrum is the definition of different “Partial Power” levels. They measure the signals frequency contribution within a given interval and represent the frequency distribution of the AE signal by more than only one characteristic value. Hence, they usually are defined for subdivisions of a certain frequency range of interest, e.g. 150 kHz intervals ranging from f_{start} = 0 kHz to f_{end} = 1200 kHz (see Appendix C in [2]).

Another sophisticated approach is to extract the frequency information from time-frequency transformations. Using such concepts based on wavelets [34] or kernel convolution procedures such as those proposed by Choi and Williams [35] this allows to obtain additional frequency features. For the discrete wavelet transformation, the intensity of the decomposition levels has been proposed as features to describe the AE signal [36], [37].

Similar as for the energetic features, established theories allow raising some expectations for the resultant frequency spectrum of a particular source mechanism in a fibre reinforced composite. All of the established theories assume a source function, which is due to a rapid internal displacement [19], [22]–[24] and has been recently confirmed by fracture mechanics

based numerical modelling [33]. Typically, this is a step function as seen exemplarily in figure 4-a for two typical rise-times. In this simple source representation, the governing factor to judge on the source dynamics is the rise-time of the internal displacement. However, the rise-time is not identical to the time the crack needs to propagate. In [2], [33] the duration for crack growth was found to be substantially shorter than the rise-time of the source function with the additional dynamics caused by inertia effects and by the vibration of the crack faces, as well as propagating surface waves. Nevertheless, a simple FFT of the two exemplary source functions of figure 4-a reveals the corresponding bandwidth of the AE source and is plotted in figure 4-b. Naturally, faster internal displacement generates broader bandwidth, i.e. causes excitation of higher frequencies. Similar, the slower internal displacement causes reduced bandwidth of the source.

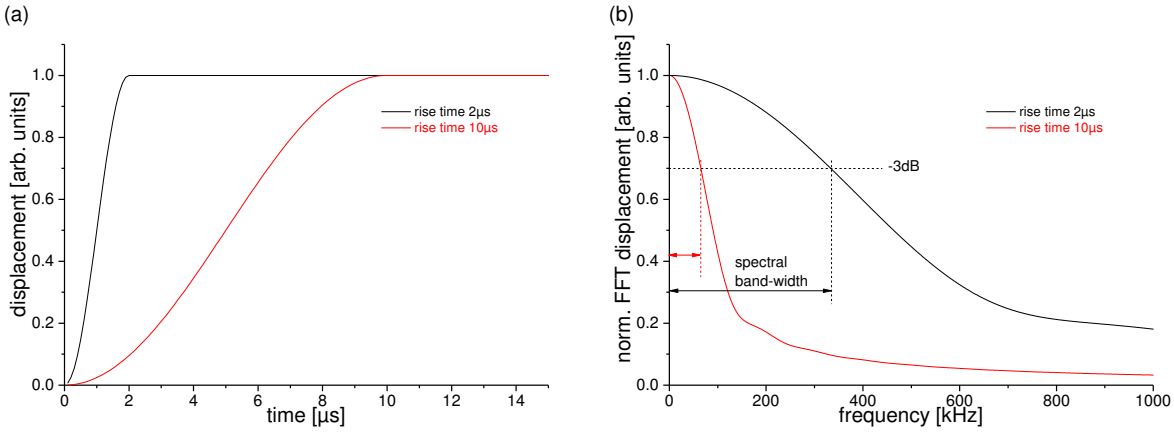

Figure 4. Scheme of source function (a) and corresponding spectral bandwidth estimated from -3dB drop (b).

4.1 Dynamics of source mechanisms in composites

Based on these considerations, the discussion now focuses on the expected dynamics for different source mechanisms. In general, the duration for a singular crack event (from initiation to rest) links to two factors. This is (i) the ductility/brittleness of the material and (ii) the geometry/extension of the crack growth. The first item directly links to the crack propagation speed. As has been discussed by Scruby [25], depending on the applied load and the material properties, cracks may potentially reach their ultimate propagation speed limit, which is the Rayleigh wave speed. The second item relates to the geometric boundary conditions posed for the crack growth. At constant speed, larger crack length will need longer to form than shorter crack length, hence adding to the overall rise-time of the source. Potentially there is a fixed upper limit to this duration of growth, as cracks in composites can be geometrically confined due to sizes of the plies or due to the overall dimension of the sample (width, thickness, …).

For failure mechanisms such as matrix cracking or delamination the basic expectation for broad crack length distributions has already been discussed in section 3.1. Based on the above considerations, this would expect a broad distribution of source rise-times for these cases.

Likewise, for discrete crack dimensions as for fibre breakage, a discrete rise-time distribution is expected.

However, reinforcement fibres such as glass or carbon fail more brittle than typical matrix polymers and also exhibit up to one order of magnitude higher Rayleigh velocities (e.g. glass 3000 m/s, carbon 5000 m/s, polymer 500 m/s) as can be calculated from the materials Young's modulus, density and Poisson's number when using the Bergman approximation [38].

Hence, generally the rise-time of the source function is significantly shorter for failure of the reinforcement fibres than for a comparable failure size of a matrix polymer. Accordingly, nominally larger crack increments as for matrix cracking and interfacial failure will reduce the bandwidth further compared to the fibre breakage bandwidth.

4.2 Transfer of frequency information from source to sensor

Although, the source dynamics govern the bandwidth of the source and the spectrum itself seems to be fairly flat with frequency (cf. figure 4-b), there are several factors which affect the propagation of frequency information from source to sensor. One example obtained from FEM calculus to demonstrate the severity of these effects shows figure 5.

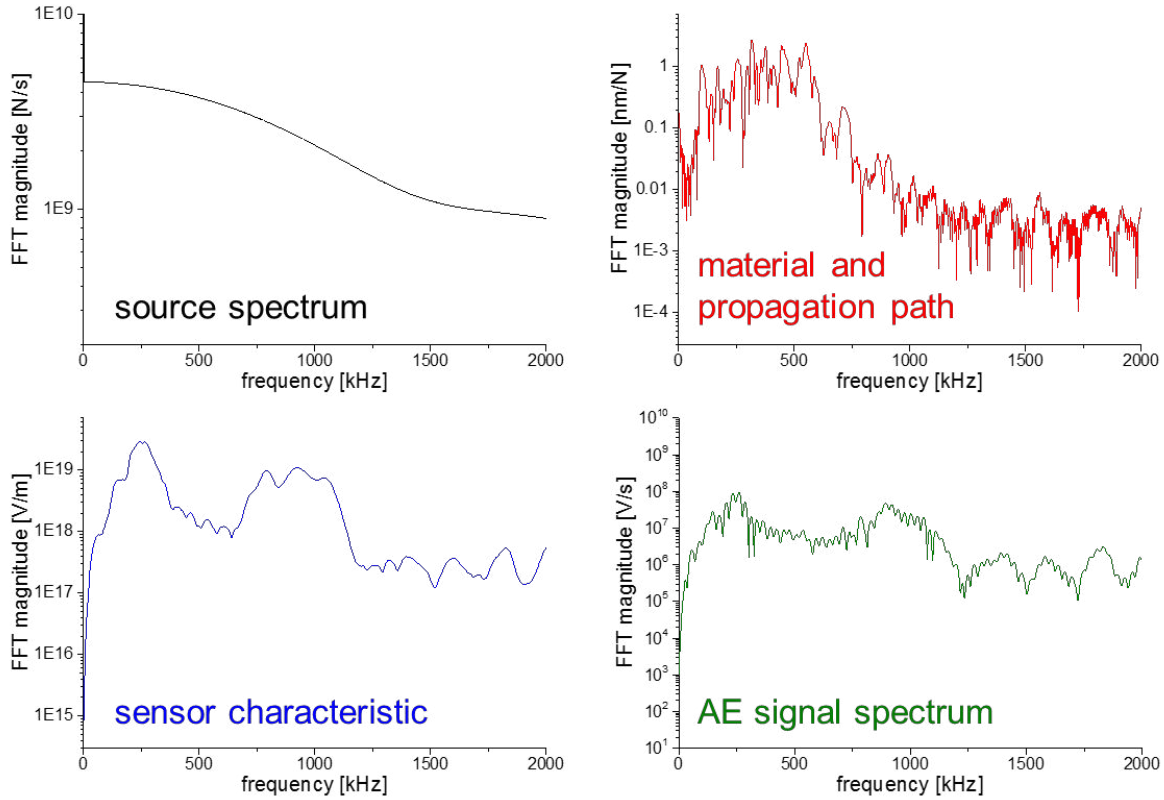

Figure 5. Transmission characteristics of sensor, material and propagation path and their influence on generation of AE signal spectrum in relation to source spectrum.

The first non-linear transmission is the formation of guided waves in a typical thin-walled composite plate. As discussed in [2], the formation of plate waves comes with particular frequency regions, that allow preferential transmission of the signal. Correspondingly, some frequency ranges transmit badly, resulting in a significant change of the frequency spectrum. The particular frequency values for preferential transmission depend mostly on the thickness of the plate and the material properties. This guided wave propagation also leads to formation of some of the characteristic peaks in the FFT spectrum of the final AE signal. Another important source of non-linear transmission is the sensing system used. Especially for the typical commercial sensor systems (resonant or multi-resonant designs), this results in additional reduction of bandwidth or may cause characteristic peaks in the frequency spectrum, which are owed to the internal sensor resonances (cf. figure 5).

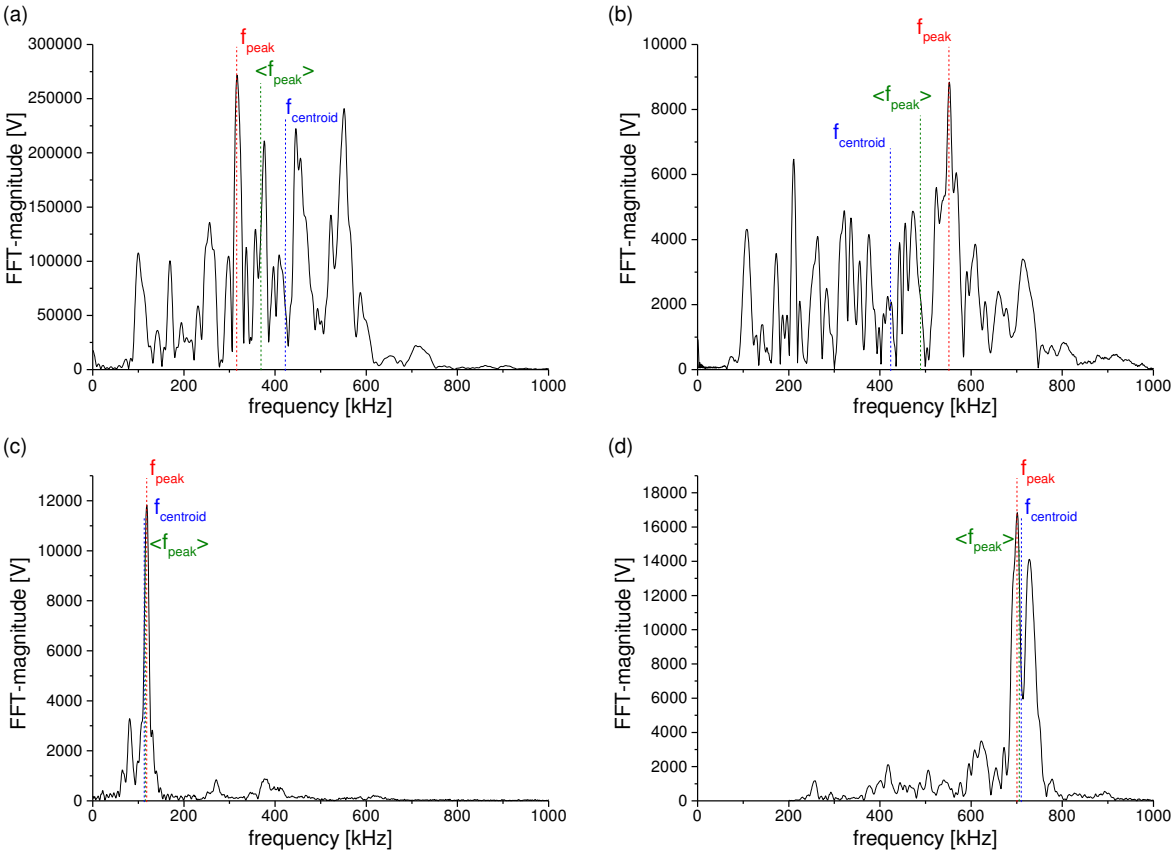

Figure 6. Comparison of frequency representation for four AE signals (a-d) using Peak-frequency f_{peak}, Frequency Centroid $f_{centroid}$ and Weighted Peak-Frequency $\langle f_{peak} \rangle$.

As seen in figure 5, the frequency information of the AE source maps not well to the acquired electrical AE signal. In particular, features such as the “Peak-frequency” usually link either to the sensor resonances or to the frequency ranges of preferential transmission of the guided waves. Thus, it does not seem appropriate to use such features to distinguish failure mechanisms based on their absolute frequency values. Typically, a choice to distinguish a mechanism of e.g. $\leqslant$ 137 kHz is either due to the sensor used or due to the material investigated.

To remove the sensor and material bias implicit to the frequency features, the use of relative features, such as the "Weighted Peak-Frequency" $\langle f_{peak} \rangle$ or "Partial Powers" was proposed [11]. As the aim of all the frequency features is to best represent the frequency spectrum, consider the four examples shown in figure 6. Visually, one would state close similarity between the spectra of figure 6-a and 6-b and high dissimilarity between spectra of figure 6-c and 6-d. Accordingly, frequency parameters should be representative numerical values for this observation. Using the f_{peak} feature this works well for the bottom case, resulting in a difference of 600 kHz. However, the upper case results in a difference of 240 kHz for visually similar spectra. Accordingly, absolute values of the f_{peak} feature do not suffice in this case.

The $f_{centroid}$ feature is less susceptible to the occurrence of peaks in the spectrum as it is obtained from an averaging of the full spectrum. However, the disadvantage of this is the reduced sensitivity to relative changes of frequency spectra. Although the example spectra of figure 6-a and 6-b are similar, they still do have different weight at low and high frequencies. Still the $f_{centroid}$ is numerically almost identical for both spectra. This lack of sensitivity of the $f_{centroid}$ feature is quite typical as the basic "finger-print" of the spectrum originates to a significant extent from constant contributions, such as sensor characteristics and guided wave propagation (cf. figure 5). Therefore, the $f_{centroid}$ feature by itself is not very useful to capture small changes relative to the average frequency content.

As result of these observations, the combination of both features into the $\langle f_{peak} \rangle$ feature was proposed [11]. As square-root combination of both other features, it retains the good discriminative capability of the f_{peak}, but is also susceptible to small changes in frequency spectrum (cf. figure 6-a and 6-b) without being too susceptible to the resonance frequencies of AE sensor or the material.

5. Conclusion

Based on the presented considerations it hardly seems applicable to perform source identification in composite materials based on energetic features unless there is a discrete size distribution expected for one mechanism. In specific cases this can be justified (i.e. matrix cracks all growing the full height and width within a ply at once). In a general situation, there is no expectation for a discrete distribution of AE signal amplitudes for one of the failure mechanisms in a composite. Instead, especially for "matrix cracking" and "interfacial failure" a wide distribution of AE signal amplitudes is expected, which cover several orders of magnitude. Thus, the AE signal amplitude and energetic features should be interpreted more in terms of strength or severity of the failure mechanism other than a feature to distinguish failure mechanisms.

In order to perform source identification, frequency features were found to provide better discriminative capabilities. The AE signals bandwidth directly relates to the duration of the crack growth. In fibre-reinforced composites, the different failure mechanisms show characteristic crack durations, which originates from the speed of the crack propagation and the typical crack length of the different mechanisms (specifically for fibre breakage). However,

the transfer of the information of the source bandwidth to corresponding AE features suffers from resonances of the structure and the sensor. To overcome the associated issues in evaluation of the frequency spectra the “weighted Peak-Frequency” was proposed. In combination with other frequency features such as the “Partial Powers” and multi-variante data analysis (e.g. by pattern recognition methods [12]) this appears as best approach to meaningful AE source identification in fibre-reinforced composites, as the reliability of a single AE feature is not significant enough to allow this complex task.

References:

[1] E. Greenhalgh, Failure Analysis and Fractography of Polymer Composites. Oxford/Cambridge/New Delhi: Woodhead Publishing Limited, 2009.
[2] M. G. R. Sause, In Situ Monitoring of Fiber-Reinforced Composites, vol. 242. Cham: Springer International Publishing, 2016.
[3] A. A. Anastassopoulos and T. P. Philippidis, “Clustering Methodology for the Evaluation of Acoustic Emission from Composites,” J. Acoust. Emiss., vol. 13, 1995.
[4] T. Philippidis, V. Nikolaidis, and A. Anastassopoulos, “Damage Characterisation of C/C laminates using Neural Network Techniques on AE signals,” NDT&E Int., vol. 31, 1998.
[5] J. M. Richardson, R. K. Elsley, and L. J. Graham, “Nonadaptive, semi-adaptive and adaptive approaches to signal processing problems in nondestructive evaluation,” Pattern Recognit. Lett., vol. 2, no. 6, 1984.
[6] E. Vi-Tong and P. Gaillard, “An algorithm for non-supervised sequential classification of signals,” Pattern Recognit. Lett., vol. 5, no. 5, 1987.
[7] S. Huguet, N. Godin, R. Gaertner, L. Salmon, and D. Villard, “Use of acoustic emission to identify damage modes in glass fibre reinforced polyester,” Compos. Sci. Technol., vol. 62, 2002.
[8] C. R. Ramirez-Jimenez, N. Papadakis, N. Reynolds, T. H. Gan, P. Purnell, and M. Pharaoh, “Identification of failure modes in glass/polypropylene composites by means of the primary frequency content of the acoustic emission event,” Compos. Sci. Technol., vol. 64, 2004.
[9] A. Marec, J.-H. Thomas, and R. Guerjouma, “Damage characterization of polymer-based composite materials: Multivariable analysis and wavelet transform for clustering acoustic emission data,” Mech. Syst. Signal Process., vol. 22, pp. 1441–1464, 2008.
[10] M. G. R. Sause, F. Haider, and S. Horn, “Quantification of metallic coating failure on carbon fiber reinforced plastics using acoustic emission,” Surf. Coatings Technol., vol. 204, no. 3, 2009.
[11] M. G. R. Sause and S. Horn, “Simulation of Acoustic Emission in Planar Carbon Fiber Reinforced Plastic Specimens,” J. Nondestruct. Eval., vol. 29, no. 2, 2010.
[12] M. G. R. Sause, A. Gribov, A. R. Unwin, and S. Horn, “Pattern recognition approach to identify natural clusters of acoustic emission signals,” Pattern Recognit. Lett., vol. 33, no. 1, 2012.
[13] D. D. Doan, E. Ramasso, V. Placet, L. Boubakar, and N. Zerhouni, “Application of an Unsupervised Pattern Recognition Approach for AE Data Originating from Fatigue Tests on CFRP,” in 31st Conference of the European Working Group on Acoustic Emission, 2014.
[14] A. A. Anastassopoulos, V. N. Nikolaidis, and T. P. Philippidis, “A Comparative Study of Pattern Recognition Algorithms for Classification of Ultrasonic Signals,” Neural Comput. Appl., vol. 8, 1999.
[15] P. Yu, V. Anastassopoulos, and a. N. Venetsanopoulos, “Pattern recognition based on morphological shape analysis and neural networks,” Math. Comput. Simul., vol. 40, 1996.
[16] F. Baensch, M. G. R. Sause, A. J. Brunner, and P. Niemz, “Damage evolution in wood – pattern recognition based on acoustic emission (AE) frequency spectra,” Holzforschung, vol. 69, no. 3, 2015.
[17] V. Kostopoulos, T. Loutas, A. Kontsos, G. Sotiriadis, and Y. Pappas, “On the identification of the failure mechanisms in oxide/oxide composites using acoustic emission,” NDT E Int., vol. 36, no. 8, 2003.
[18] R. de Oliveira, O. Frazão, J. L. Santos, and A. T. Marques, “Optic fibre sensor for real-time damage detection in smart composite,” Comput. Struct., vol. 82, no. 17–19, 2004.
[19] M. Giordano, L. Condelli, and L. Nicolais, “Acoustic emission wave propagation in a viscoelastic

plate," Compos. Sci. Technol., vol. 59, 1999.
[20] J. Bohse, "Acoustic emission characteristics of micro-failure processes in polymer blends and composites," Compos. Sci. Technol., vol. 60, 2000.
[21] B. S. Everitt, Cluster Analysis, 3rd ed. John Wiley & Sons Inc., New York, 1993.
[22] M. V. Lysak, "Development of the theory of acoustic emission by propagating cracks in terms of fracture mechanics," Eng. Fract. Mech., vol. 55, no. 3, 1996.
[23] M. Ohtsu and K. Ono, "A generalized theory of acoustic emission and Green's function in a half space," J. Acoust. Emiss., vol. 3, 1984.
[24] M. Ohtsu and K. Ono, "The generalized theory and source representation of acoustic emission," J. Acoust. Emiss., vol. 5, 1986.
[25] C. B. Scruby, "Quantitative acoustic emission techniques," Nondestruct. Test. Vol. 8, 1985.
[26] A. E. Green and W. Zerna, Theoretical Elasticity. New York, USA: Oxford University Press, 2002.
[27] M. G. R. Sause and A. Monden, "Comparison of Predicted Onset of Failure Mechanisms By Nonlinear Failure Theory and By Acoustic Emission Measurements," in 16th European Conference on Composite Materials, 2014.
[28] C. B. Scruby, H. N. G. Wadley, and J. J. Hill, "Dynamic elastic displacements at the surface of an elastic half-space due to defect sources," J. Phys. D. Appl. Phys., vol. 16, no. 6, 2000.
[29] S. O. Gade and M. G. R. Sause, "Measurement and Study of Electromagnetic Emission Generated by Tensile Fracture of Polymers and Carbon Fibres," J. Nondestruct. Eval., vol. 36, no. 1, 2017.
[30] S. Lomov, M. Karahan, A. Bogdanovich, and I. Verpoest, "Monitoring of acoustic emission damage during tensile loading of 3D woven carbon/epoxy composites," Text. Res. J., vol. 84, no. 13, 2014.
[31] Y. Swolfs, I. Verpoest, and L. Gorbatikh, "Issues in strength models for unidirectional fibre-reinforced composites related to Weibull distributions, fibre packings and boundary effects," Compos. Sci. Technol., vol. 114, 2015.
[32] A. E. Scott, M. Mavrogordato, P. Wright, I. Sinclair, and S. M. Spearing, "In situ fibre fracture measurement in carbon-epoxy laminates using high resolution computed tomography," Compos. Sci. Technol., vol. 71, no. 12, Aug. 2011.
[33] M. G. R. Sause and S. Richler, "Finite Element Modelling of Cracks as Acoustic Emission Sources," J. Nondestruct. Eval., vol. 34, no. 1, 2015.
[34] M. A. Hamstad, "Comparison of Wavelet Transform and Choi-Williams Distribution to Determine Group Velocities For Different Acoustic Emission Sensors," J. Acoust. Emiss., vol. 26, 2008.
[35] H.-I. Choi and W. Williams, "Improved Time-Frequency Representation of Multicomponent Signals Using Exponential Kernels," IEEE Trans. Acoust. Speech Signal Process., vol. 37, no. 6, 1989.
[36] L. Angrisani, P. Daponte, and M. D'Apuzzo, "A method for the automatic detection and measurement of transients. Part I: the measurement method," Measurement, vol. 25, no. 1, 1999.
[37] G. Qi, A. Barhorst, J. Hashemi, and G. Kamala, "Discrete wavelet decomposition of acoustic emission signals from carbon-fiber-reinforced composites," Compos. Sci. Technol., vol. 57, 1997.
[38] R. H. Bergman, R. A. Shahbender, E. H. Bergman, R. A. Shahbender, R. H. Bergman, and R. A. Shahbender, "Effect of Statically Applied Stresses on the Velocity of Propagation of Ultrasonic Waves," J. Appl. Phys., vol. 29, no. 12, p. 1736, Jun. 1958.